HIGH RESOLUTION X-RAY SPECTROSCOPY CLOSE TO ROOM TEMPERATURE

L. Strüder, N. Meidinger, D. Stötter
MPI für extraterrestrische Physik, Halbleiterlabor,
Paul-Gerhardt-Allee 42, D – 81245 München, Germany

J. Kemmer, P. Lechner P. Leutenegger, H. Soltau
KETEK GmbH, Am Isarbach 30, D – 85764 Oberschleißheim, Germany

F. Eggert, M. Rohde, T. Schülein
RÖNTEC GmbH, Rudower Chaussee 6, 12489 Berlin, Germany

July 1998

A b s t r a c t

Originally designed as position sensitive detectors for particle tracking, silicon drift detectors are nowadays used for high count rate X-ray spectroscopy, operating close to room temperature. Due to their low capacitance read-node concept, they belong to the fastest high resolution detector systems. They have opened a new spectrum of experiments in the wide field of X-ray spectroscopy: fluorescent analysis, diffractometry, material analysis, synchrotron experiments like X-ray holography and element imaging in scanning electron microscopes. The fact, that the detector system can be used at room temperature with good spectroscopic performance, and at -10°C with excellent energy resolution, avoiding liquid nitrogen for cooling and high quality vacuum, guarantees a large variety of new applications, independent of the laboratory environment.

A brief description of the device principles is followed by basics on low noise amplification. The performance figures of a complete detector system are presented as well as some dedicated applications already realized. The use in a surface mapping instrument will be described as well as a recently operated "mini-spectrometer" for the analysis of works of art.

For the European X-ray Multi-Mirror mission (XMM) and the German X-ray satellite ABRIXAS fully depleted pn-CCDs have been fabricated, enabling high speed, low noise, position resolving X-ray spectroscopy. The detector was designed and fabricated with a homogeneously sensitive area of 36 cm^2 . At -70°C it has a noise of 4 e^- rms, with a readout time of the total focal plane array of 4 ms. The maximum count rate for single photon counting was 10^5 cps under flat field conditions. In the integration mode more than 10^9 cps can be detected at 6 keV. Its position resolution is in the order of 100 μm. The quantum efficiency is higher than 90% ranging from Carbon K X-rays (277 eV) up to 10 keV.

1 The Silicon Drift Detector Principle

In 1983 Gatti and Rehak proposed a new detector scheme based on sideward depletion [5]. The idea is that a large semiconductor wafer of high resistivity e.g. n-type silicon can be fully depleted by a small n^+ ohmic contact positively biased with respect to the p^+ contacts covering both surfaces of the silicon wafer.

In the standard configuration the depletion zones will expand from all rectifying junctions simultaneously as long as the ohmic access from the n^+ anode to the entire (non-depleted) bulk is not interrupted. At a given voltage the depletion zones propagating from the p^+ areas touch each other. Under this condition the former conducting electron channel symmetrically located in the middle of the substrate between the p^+ implants will abruptly disappear. At this moment the depletion of the whole wafer is completed at a voltage which is four times lower than the voltage needed to deplete a simple diode of the same thickness. Under the above described condition the electron potential energy in a section perpendicular to the wafer surface has a parabolic shape, with an electron potential minimum in the middle of the wafer.

The silicon drift detector (SDD) is derived from this principle of sideward depletion by adding an electrical field parallel to the surface. This is simply achieved by a segmentation of both or one of the p^+ areas to form a strip pattern and superimposing a voltage gradient on the strip system. The direction of the voltage gradient is such that the n^+ readout anode is the point of minimum potential energy for electrons and therefore collecting all signal electrons generated in the depleted volume.

The main advantage of the SDD compared to a standard diode of equal size is the small value of the anode capacitance which is practically independent of the total area of the device. This feature translates in a shorter rise time and bigger amplitude of the output signal for a given amount of collected electrons, i.e. the signal is less subject to noise of subsequent electronic components. The charge collection time of about 100 ns from the edge of the detector is disadvantageous. However the time spread of the charge cloud is only in the order of 5 ns. Overlapping charge clouds limits the single photon counting capability.

With the SDD principle the designer has great flexibility in the choice of anode configurations and drift directions. For instance at the semiconductor laboratory of the Max-Planck-Institutes (MPI-HLL) large SDDs have been fabricated with linear drift geometry, i.e. parallel strips [4], up to 4.2× 3.6 cm^2 and a 55 cm^2 cylindrical geometry on 4 inch wafers, in which electrons drift along the radial direction to one of 360 anodes placed at the wafer edge [8]. Both systems have been used as particle trackers. In this mode of operation the position of the interacting particle is reconstructed by a measurement of the electrons' drift time.

2 Silicon Drift Detectors for X-ray Spectroscopy

In an advanced design, optimised for applications in X-ray spectroscopy and also realised by MPI-HLL, the strip system at one side has been replaced by a large area pn-junction, which is used as a homogeneous, very thin entrance window for the radiation [9], [3]. The electric field is generated by concentric cylindrical drift electrodes on the opposite side of wafer forcing the signal electrons to a small sized anode in the center of the device. The potentials of the individual drift electrodes are defined by an integrated voltage divider, i.e. only the first and last p^+ ring must be contacted

and biased externally (Fig. 1).

The electron potential of the cylindrical silicon drift detector is shown in Fig. 2 in a section perpendicular to the surface through the silicon wafer. It shows the potential energy for electrons of the device of Fig. 1 in operating condition including all field strips and the central electron collecting anode. The equipotential of the homogeneously doped radiation entrance window can be seen on the back, the field strips with their decreasing (negative) potential on the front side. There is no field free region in the device and all electrons in the sensitive area are guided within less than 100 ns towards the readout node.

The anode not only collects signal electrons generated by the absorption of radiation but also electrons which have been thermally generated within the depleted volume. The latter electrons make up a statistically varying leakage current and spoil the signals. Due to the elaborated process technology at MPI-HLL the rate of thermal generation of charge carriers is so small that the device can be operated at moderate low temperature or without cooling at all.

3 On-Chip Amplification

The anode is connected to an amplifying junction field effect transistor (JFET) integrated directly on the detector chip (see Fig. 1). This way not only the capacitance of the detector-amplifier system is minimized by eliminating bond wires between detector and amplifier, thus avoiding all kinds of stray capacitances between the readout node and ground, making the system again faster and less noisy. Further advantages are evident as the effect of electrical pickup is significantly reduced and problems of microphony, i.e. noise by mechanical vibration, are excluded.

With the help of Fig. 1 the basics of the amplification process of the integrated FET can be easily understood. In the center of the schematic drawing a single sided JFET is shown. Let's assume that electrons, generated by the ionizing radiation drift towards the readout anode. The voltage generated at the read-out node is directly coupled to the p^+ gate of the n-channel transistor (source and drain are n^+ implants, the transistor channel is a deep n implant). The negative voltage on the p^+ gate reversely biases the junction, thus depleting the transistor channel, resulting in a current drop through the transistor. This change of current can be precisely measured.

As it collects more and more electrons the FET gate gets increasingly reverse biased relative to the transistor channel. At a given potential difference the gate is discharged by a breakdown of the gate-channel junction at the drain end of the channel. During detector operation the gate adjusts its potential in a way that all signal and leakage current electrons are compensated by the breakdown mechanism. In other words: the integrated FET resets itself, there is no need for an externally clocked reset pulse, and the SDD is operated with dc voltages only.

4 Silicon Drift Detector Systems

A short summary of the SDD characteristics will lead us to new applications which have been initiated and made possible by this detector type:

We have designed, fabricated and tested cylindrical drift detectors with integrated FET as shown in Fig.1 [7]. They have an active area of 5 mm^2 and a thickness of 300 μm. At room temperature the intrinsic noise figures are in the order of 15 e^- translating in a width of the ^{55}Fe

Mn K_α line (5.9 keV) of 180 eV at a shaping time of 0.25 μs (see Fig. 3). The bulk leakage current at 300 K contributing to the system noise is less than 1 nA per cm^2 . At 263 K, a temperature that can be gained by a single stage Peltier cooler, the equivalent noise charge is reduced to about 9 e^- rms, i.e. 140 eV FWHM at Mn K_α line. At 243 K the SDD is already as good as conventional Si(Li) or HPGe detectors requiring a cooling around 100 K.

On the other hand the SDD is operated at shaping times in the order of 100 ns while conventional systems with comparable spectroscopic quality need longer time constants at least by a factor 100. That means that the SDD can be operated at extremly high count rates which are beyond the potentialities of other systems: Up to 10^5 cps incoming counts can be detected without a significant increase in the equivalent noise charge (see fig. 10), that means without a broadening of the e.g. Mn K_α line of the ^{55}Fe spectrum. At 6×10^5 cps the resolution is still as good as 230 eV FWHM at the Mn K_α line.

The radiation entrance window has been optimized for the detection of soft X-rays: the quantum efficiency is 90% at 0.5 keV and above 90% between 1 keV and 10 keV [12], [13]. All other detector relevant parameters are satisfactory: complete charge collection, spatially homogeneous response, reproducibility and longterm stability.

These figures recommend the use of SDDs in two categories of applications:

(1) high count rate applications

Silicon drift detectors have been installed as radiation monitors in our satellite test facility PANTER, and they have been operated in EXAFS and atomic holography at various synchroton light sources [6]. These experiments take profit of the SDD's high rate capability, still with simultaneous good energy resolution, thus reducing necessary beam time and related costs by orders of magnitudes.

For synchrotron applications we also designed and produced detector arrays by combinig several SDDs to a multi-cell drift detector. This way deliberately large sensitive areas can be achieved without loosing the high count rate capability and the low noise level of the individual 5 mm^2 large subsystems. The largest device has 39 readout nodes corresponding to 195 mm^2 area (see Fig. 4). Multiplexing VLSI amplifiers are actually being developed to keep the complexity of the readout electronics for the user at a reasonable level.

(2) compact, easy-to-use setup

That fact that SDDs don't require cooling by liquid nitrogen or cryogenic systems allows the integration of detector, Peltier cooler, and Be entrance window in a small sized package. This compact, inexpensive module is well suited for a number of commercial applications and on-the-field measurements:

SDDs have already been used as X-ray detectors for electron microbeam analysis in scanning electron microscopes [14]. In this setup the electron beam is used not only to produce a surface image of the sample but also as generator of characteristic X-rays which are detected by the SDD and yield information of the chemical consistence of the sample.

The SDD module in combination with a commercial microfocus X-ray tube makes up a compact, portable spectrometer for X-ray fluorescence (XRF) measurements, also on the field, i.e. independent of laboratory infrastructure. This feature already led to the use of such a spectrometer in archeometry. In this context it is now possible to perform a fast element analysis of works of art in galleries and museums without transportation of the precious objects to scientific laboratories.

5 Works of Art Investigations with Silicon Drift Detectors

In archeometry different kinds of investigations are used for the characterization of art objects. In particular, the XRF (X-Ray Fluorescence) spectroscopy is a non-destructive technique widely used for the identification of chemical elements in pigments, metal alloys, and other materials. The classical high resolution cryogenic detectors, like Si(Li) and HP(Ge) detectors (whose energy resolution is of the order of 140 eV FWHM at the Mn K_α line), are not completely suitable for the realization of portable instrumentation because of the need of liquid nitrogen in the cooling system.

Recently new silicon PIN diodes simply cooled by a Peltier element have been introduced. Their energy resolution (of the order of 250 eV FWHM at the Mn K_α line) is in some cases unsatisfactory (especially for the analysis of light chemical elements). At low energy, the main contribution to the FWHM is due to the electronic noise of the detector front-end system, which is associated to the detector-capacitance, directly dependent on the detection area. This performance is only obtained with a PIN type detector at very low count rates, typically 1000 cps.

The possibility to operate the SDD at non cryogenic temperatures and the excellent energy resolution (of the order of 150 eV FWHM at 6 keV) makes these detectors suitable for the realization of high resolution portable instrumentation. Recently a portable high resolution x-ray spectrometer - based on the Silicon Drift Detector, cooled by a Peltier element - was realized at the research laboratories of Politecnico di Milano [1]. A commercial miniaturized X-ray tube was utilized as an excitation source. The measurements on different kinds of art objects confirmed the ease of use combined with the high class performance, in particular the high energy resolution. Fig.5 shows a spectrum of an orange pigment recorded with the above described system. The almost background-free detection of the individual chemical elements helps to identify the composition of complex materials directly at the location of the work of art. Thus a transfer of the objects in the laboratory is not longer needed.

6 Element Imaging in Electron Microscopes with Silicon Drift Detectors

Silicon drift detectors have been tailored to use them as energy dispersive spectrometers in scanning electron microscopes. The RÖNTEC-XFlash^{TM} system was developed to record at temperatures achievable with single stage Peltier cooler, X-ray fluorescence spectra at about 10 times higher count rates than conventional energy dispersive x-ray spectrometers. This results in spatially resolved element mapping with a high dynamic range, i.e. several hundred grey levels with short measurement times. Fig. 6 shows the analysis of a meteorite with a spatial resolution of 280×224 pixels. The measuring time was 10 minutes and the average X-ray count rate was 250,000 counts per second. The RÖNTEC-MAX^{TM} pulse processer system was used for the data aquisition, the images were processed with a system from Point Electronic. The upper left is the scanning electron image, the others show Se, Fe, Mo, Ni, Ca and Mg, as distributed in the images. Compared to conventional EDX systems, a factor of 10 is gained in the number of grey steps. Another factor of 4 in count rate capability can be obtained by further improvements of the pulse processing electronics.

In Fig. 7 a comparison is shown between a conventional EDX system, a high end digital pulse processor based system and The RÖNTEC-XFlash^{TM} system. The number of grey levels in an

conventional high end EDX system operating at 20 kcps is 22 for a measuring time of 10 minutes. A state-of-the-art system with a digital pulse processor achives with 50 kcps 58 grey steps, while the RÖNTEC MultiMAX^{TM} system reaches 236 grey steps in the same measurement. The XFlash^{TM} detector system was operated at -10°C while the conventional systems were run at liquid nitrogen temperatures. The integration of the first amplifying stage adds the advantage of being completely insensitive to all kind of accoustic (microphonic) noise.

7 Fully Depleted Charge Coupled Devices (pn-CCDs)

For ESA's X-ray Multi Mirror mission, to be launched in the year 1999 we have developed a 6× 6 cm^2 large monolithic X-ray CCD [10] with high detection efficiency up to 15 keV, low noise level (ENC $\approx$ 5e$^-$) and an ultrafast readout time of 4 ms. A schematic cross section, already showing some of the advantages of the concept is displayed in Fig. ??. The concept allows for an optimum adaption of the pixel size to the X-ray optics, varying from 30 μm up to 300 μm pixel size. The energy response is higher than 90% at 10 keV because of the sensitive thickness of 300 μm . The low energy response is given by the very shallow implant of the p$^+$ back contact; the effective "dead" layer is smaller than 150 Å [11]. The good time resolution is given by the parallel readout of 64 channels. A high radiation hardness is built in by avoiding MOS structures and by the fast transfer of the charge in a depth of more than 10 μm. The spatially uniform detector quality over the entire field of view is realized by the monolithic fabrication of 12 individually operated 3× 1 cm^2 large pn-CCDs on a single wafer. As the telescope system resolution on XMM is in the order of 15 arcsec with a focal length of about 7.5 m, the extension of a point source in the X-ray sky is about 500μm in the focal plane. That is why a pixel size of 150× 150 μm^2 for the CCDs was chosen.

The best values for the readout noise of the on-chip electronics is 3 e$^-$ rms at 150 K, typical values scatter around 4 - 5 e$^-$ rms. The charge transfer properties are as good as in standard CCDs, in the order of a few % charge loss from the last to the first pixel over a distance of 3 cm charge transfer. Fig. 9 (a) shows a ^{55}Fe spectrum of a pn-CCD in a flat field measurement resulting in a typical energy resolution of 130 eV (see Fig. 9) to 140 eV (FWHM) [12]. The impact of the material properties of silicon and related impurities and their consequences for the operation of scientific grade X-ray pn-CCDs including the effects of radiation damage, is treated in detail in [13].

In a single photon counting mode the quantum efficiency was measured with respect to a calibrated position sensitive proportional counter. In addition, a dc photo current measurement at the BESSY synchrotron in Berlin with a calibrated monochromator and reference detector is shown. The part (b) of figure 9 shows the single photon counting data (× signs) and the dc photocurrent results in steps of 5 eV from 60 eV up to 3 keV. The single photon data were taken with the C_K, O_K, $Cu_{L\alpha}$, $Ti_{K\alpha}$, $Cu_{K\alpha}$ and $Cu_{K\beta}$ from an X-ray tube [2]. The quantum efficiency on the low energy side was further improved with respect to the measurements in Fig. 9 shown above by increasing the drift field at the p$^+$ junction entrance window [14]. The read out electronics of the pn-CCD system is described in [10]. A charge sensing amplifier followed by a multicorrelated sampling stage, multiplexer and output amplifier (CAMEX64B JFET/CMOS chip) guide the pn-CCD pixel content as a voltage signal to a 10 MHz 12 bit flash ADC system. The whole system, i.e. CCD and CAMEX64B amplifier array dissipate a power of 0.7 W a value which is tolerable

for the XMM satellite mission. A further increase of the readout speed can be made only on the expense of further increase of power, or a degradation of the noise performance.

We have tested the pn-CCD system in a single photon counting mode in flat field conditions at high count rates. If signal pile-up must be avoided, that means, only one photon is allowed in one pixel, the maximum photon count rate is approximately 3,000 counts per cm^2 and second, leading to 10^5 counts per second (cps) for the full detector system. This experiment was done with a mechanical chopper wheel, preventing photons hitting the CCD during readout. The open position on the chopper wheel added another 6 ms of "photon integration time" to the 4 ms readout time. Split events, i.e. events with electrons in more than one pixel, originating from one single photon, were reconstructed and summed to one photon event. In total, 75% of all events are single pixel events, 23% are two pixel events and 2% are events with three and four pixels involved. One single X-ray hit never affects more than four pixels.

The charge handling capacity of the individual pixels was tested with the 5.486 MeV alpha particles from a radioactive ^{241}Am-source. More than 2×10^6 electrons can be properly transfered in every pixel.

8 COUNT RATE CONSIDERATIONS

In principle, a pixel detector, where every sensitive cell has its own amplifier and read-out chain would be the fastest device for high resolution X-ray spectroscopy. But up to now no system is operational with properties which match the requirements for spectroscopic applications. The main limitations arise from the power consumption, and if the first amplification is not directly performed in the detector, from the noise performance of highly integrated analog external circuits.

The silicon drift detectors and fully depleted, backside illuminated pn-CCDs transfer the charges over larger distances to a readout node coupled to the gate of a junction field effect transistor (JFET). While the pn-CCD guides the signal charges – discretly in time – to the read node, this is done continuously in a silicon drift detector. Therefore the position resolution in a cylindrical SDD with one read-out node in the center is as large as the area of the drift fields expand (in our case about 2 mm), while in the CCD the spatial resolution is given by the pixel size. That's why the count rate capabilities for single photon counting are quite different.

8.1 Count rate capabilities of the pn-CCD system

The pn-CCD system for the XMM satellite was not designed for high count rates but for high time resolution. Special operation modes were implemented (e.g. window modes, timing modes) to reduce the sensitive area to the benefit of a faster readout.

First we consider the full frame readout of the largest possible area (40 cm^2). In order to keep pile up below 5%, we can process about 500 photons per frame and per cm^2. If the full position resolution is required, a mechanical shutter can prevent radiation to hit the detector during readout. In this case, 10 ms are needed to completely readout the system, i.e. at best, 5×10^4 events can be detected in the single photon counting mode per cm^2 and second. This finally leads to about 2×10^6 photons per second for the whole system maintaining to full spatial resolution. Locally, but not for the whole system the count rate per area can be increased by using the CCD as an analog storage in the so-called windowing and timing modes [15].

If no single photon counting is required and the CCD is used as a imager instead of a photon counter, the count rate can be increased dramatically, e.g. by three orders of magnitude for 3 keV photons.

8.2 Count rate capabilities of the silicon drift detector

As shown in Fig.10, each cell of the silicon drift detector can process approximately 10^5 events per second, if operated at room temperature. The increase of the FWHM at higher rates is mainly due to the processing electronics not yet due to the detector properties. The actual size of a SDD cell is 5 mm^2. This translates to a count rate of 2×10^6 per cm^2 and second in a single photon counting spectroscopic read-out mode.

For an experiment in X-ray holography a 1,000 cell detector will be built, equipped with low-noise front end JFET-CMOS VLSI electronic, comparable with the CAMEX64B amplifier being used with the pn-CCD. Such a system will have a total sensitve area of 50 cm^2 and a system count rate capability of more than 10^8 counts per second.

9 Summary

We have demonstrated the performance of high resolution spectrometers, which can be operated at or close to room temperature avoiding liquid nitrogen for cooling and vacuum environment. The spectrometers are compact and with count rate capabilities which are 10 times higher than conventional systems. The cost of the spectrometer is significantly lower than comparable conventional Si(Li) or high purity germanium systems.

Silicon drift detector based spectrometers have been used as fast detectors in synchrotron experiments, as XRF devices for investigations in archeometry, in the field of microbeam analysis in scanning electron microscopes and for the scintillation light readout when coupled to anorganic scintillators. New scientific and industrial applications have already been proposed.

Fully depleted, back side illuminated pn-CCDs with a sensitive area of 36 cm^2 have been fabricated and tested. From infrared light up to 15 keV X-rays they perform with high efficiency, high speed and excellent spectroscopic and imaging properties. They are operated at temperatures around -80°C .

10 ACKNOWLEDGEMENTS

The author thanks the staff of the MPI Halbleiterlabor and the Max-Planck-Institute für Physik und extraterrestrische Physik for their continuous support. The perfect mounting and bonding of the devices by P. Solc and S. Kemmer is acknowledged. This research is supported by the German space agency DARA, the European Space Agency and the HCM program of the European Community.

References

[1] A. Longoni and C. Fiorini and P. Leutenegger and S. Sciuti and G. Fronterotta and L. Strüder and P. Lechner . A portable XRF spectrometer for non-destructive analysis in archeometry . NIM A, 409(1):395 – 400, 1998.

[2] H. Soltau, P. Holl, S. Krisch, C.v. Zanthier, D. Hauff, R. Richter, H. Bräuninger, R. Hartmann, G. Hartner, N. Krause, N. Meidinger, E. Pfeffermann, C. Reppin, G. Schwaab, L. Strüder, J. Trümper, E. Kendziorra, J. Krämer . Performance of the pn-CCD X-ray Detector System Designed for the XMM Satellite Mission. NIM A, 377(340 – 345), 1996.

[3] P. Lechner, S. Eckbauer, R. Hartmann, R. Richter, L. Strüder, S. Krisch, H. Soltau, D. Hauff, C. Fiorini, E. Gatti, A. Longoni, M. Sampietro . Silicon Drift Detectors for high resolution room temperature X-ray Spectroscopy . NIM A, 377:346 – 351, 1996.

[4] E. Gatti, A. Longoni, M. Sampietro, P. Giacomelli, A. Vacchi, P. Rehak, J. Kemmer, P. Holl, L. Strüder, and W. Kubischta. Silicon Drift Chamber Prototype for the Upgrade of the UA 6 Experiment at the CERN pp Collider. NIMA, 273:865 – 868, 1988.

[5] E. Gatti and P. Rehak. Semiconductor drift chamber - an application of a novel charge transport scheme. NIMA, 225:608 – 621, 1984.

[6] Ch. Gauthier, J. Goulon, E. Moguiline, A. Rogalev, P. Lechner, L. Strüder, C. Fiorini, A. Longoni, M. Sampietro, A. Walenta, H. Besch, H. Schenk, R. Pfitzner, U. Tafelmeier, K. Misiakos, S. Kavadias, and D. Loukas. A High Resolution, 6-Channel – Silicon Drift Detector Array with Integrated JFET's Designed for EXAFS: First X-Ray Fluorescence Excitation Spectra Recorded at the ESRF. NIM A, 382:524 – 532, 1996.

[7] R. Hartmann, D. Hauff, S. Krisch, P. Lechner, G. Lutz, R. H. Richter, H. Seitz, L. Strüder, G. Bertuccio, L. Fasoli, C. Fiorini, E. Gattiand A. Longoni, E. Pinotti, and M. Sampietro. Design and test at room temperature of the first silicon drift detector with on-chip electronics. In IEDM Technical Digest, pages 535 – 539, 1994.

[8] P. Holl, P. Rehak, F. Ceretto, U. Faschingbauer, J.P. Wurm, A. Castoldi, and E. Gatti. A 55 cm^2 cylindrical silicon drift detector. NIMA, 377:367 – 374, 1996.

[9] J. Kemmer, G. Lutz, E. Belau, U. Prechtel, W. Welser . Low Capacity Drift Diode. NIM A, 253:378 – 381, 1987.

[10] E. Kendziorra, E. Bihler, B. Kretschmar, M. Kuster, B. Pflüger, R. Staubert, H. Bräuninger, U. Briel, E. Pfeffermann, and L. Strüder. PN-CCD camera for XMM: Performance of high time resolution - bright source modes . SPIE, 3114, 1997.

[11] N. Meidinger, L. Strüder, Heike Soltau and C.v. Zanthier . Radiation Hardness of pn-CCDs for X-ray Astronomy. IEEE - NS, 42(6):2066 – 2073, 1995.

[12] R. Hartmann, D. Hauff, P. Lechner, R. Richter, L. Strüder, J. Kemmer, S. Krisch, F. Scholze, G. Ulm . Low Energy Response of Silicon pn-junction Detectors. NIM A, 377:191 – 196, 1996.

[13] R. Hartmann, L. Strüder, J. Kemmer, P. Lechner, O. Fries, E. Lorenz, R. Mirzoyan . Ultrathin Entrance Windows for Silicon Drift Detectors . NIM A, 387(1,2):241, 1997.

[14] RÖNTEC GmbH, Rudower Chaussee 6, Geb. 19.1/2, D – 12489 Berlin . X-flash detektor. Product Information, 1.1(4), March 1997.

[15] L. Strüder, H. Bräuninger, M. Meier, P. Predehl, C. Reppin, M. Sterzik, J. Trümper, P. Cattaneo, D. Hauff, G. Lutz, K.F. Schuster, A. Schwarz, E. Kendziorra, A. Staubert, E. Gatti, A. Longoni, M. Sampietro, V. Radeka, P. Rehak, S. Rescia, P.F. Manfredi, W. Buttler, P. Holl, J. Kemmer, U. Prechtel, and T. Ziemann. The MPI/AIT X-ray imager – High speed pn-CCDs for X-ray detection. NIMA, 288:227 – 235, 1990.

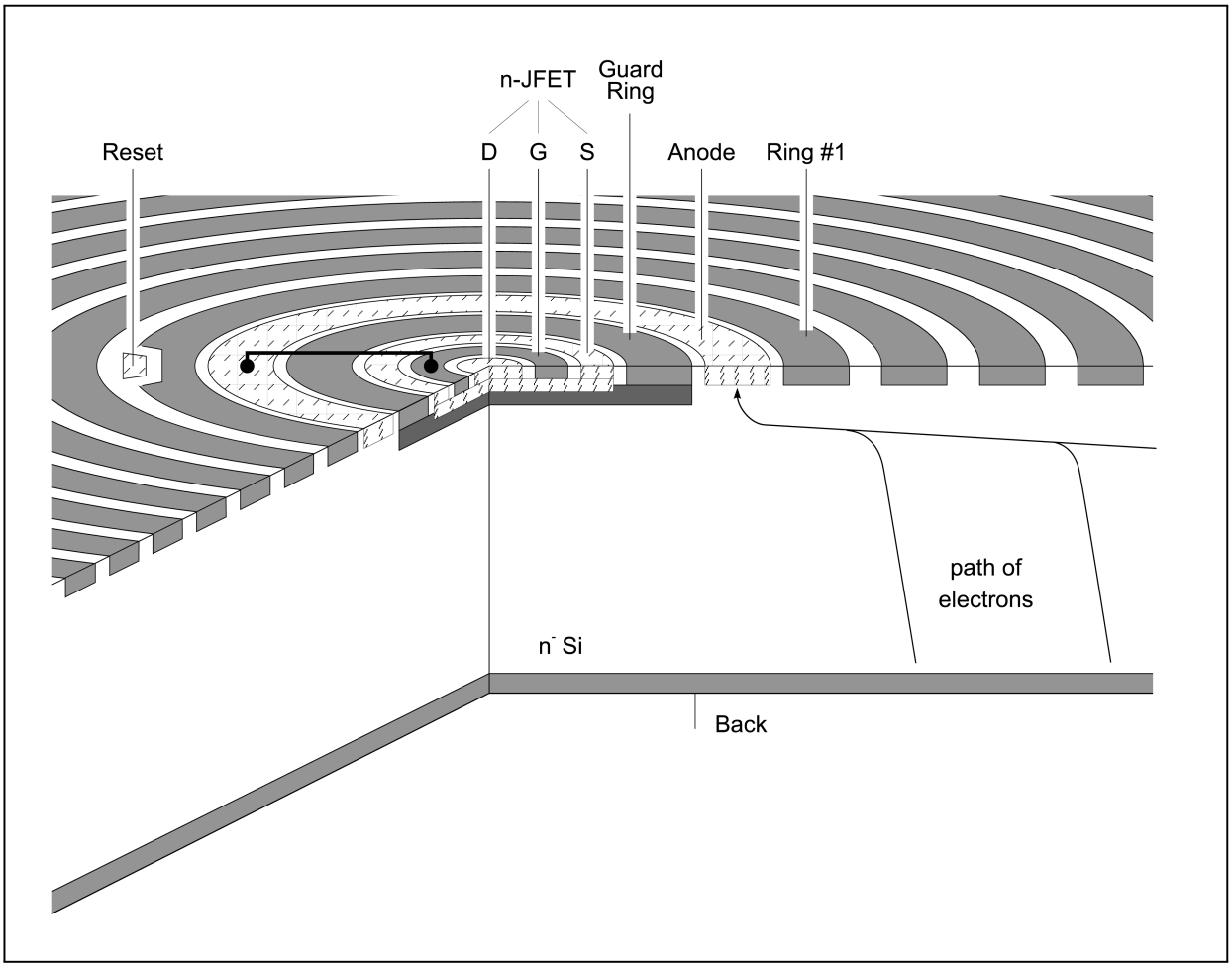

Figure 1: Central area of a cylindrical silicon drift detector with an integrated amplifier for spectroscopic applications. The entire silicon wafer is sensitive to radiation.

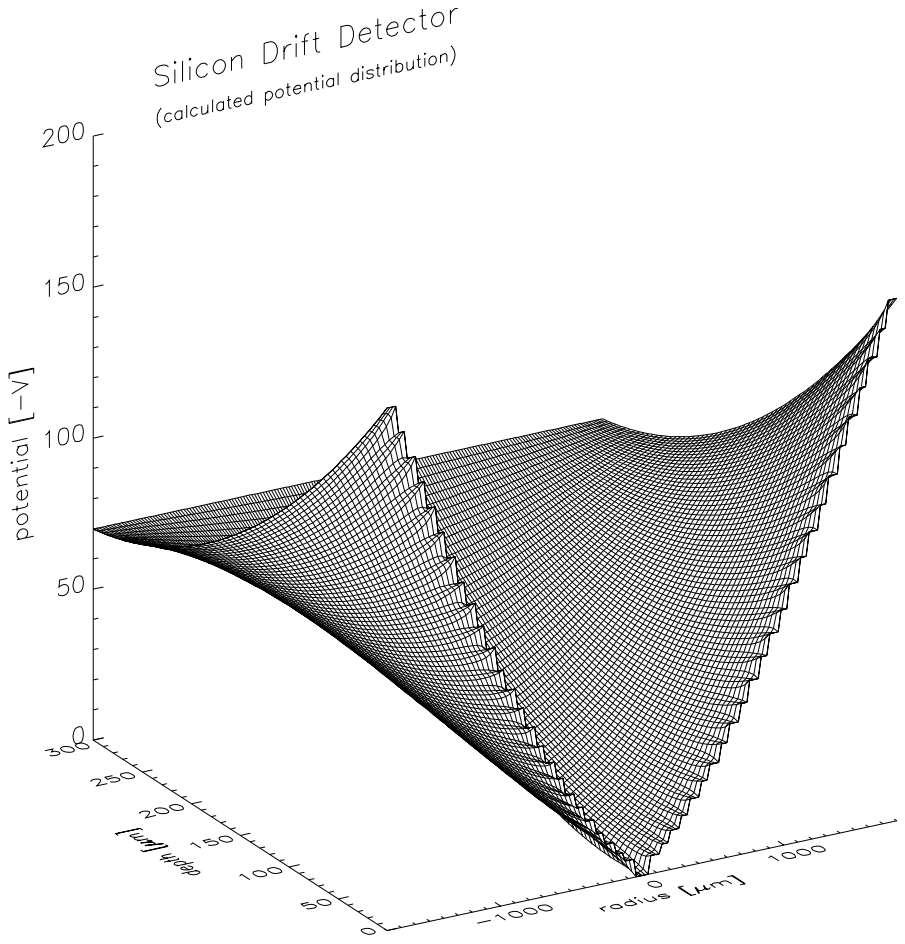

Figure 2: Potential energy distribution in a silicon drift detector. The simulation applies to the whole detector shown in Fig. including the electron collecting readout node.

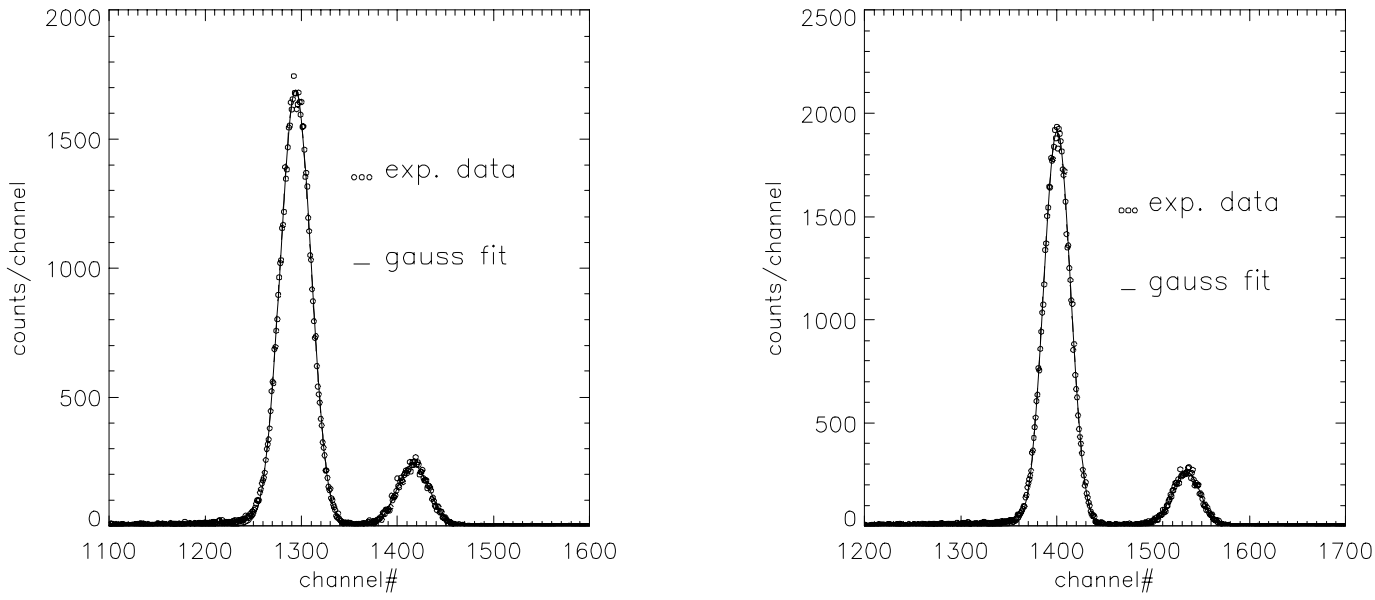

Figure 3: (a) Manganese spectrum recorded with a SDC at 25 °C. The shaping time was 0.25μs, the FWHM is 178 eV.
(b) Manganese spectrum recorded with a SDC at -13 °C. The shaping time was 1μs, the FWHM is 144 eV.

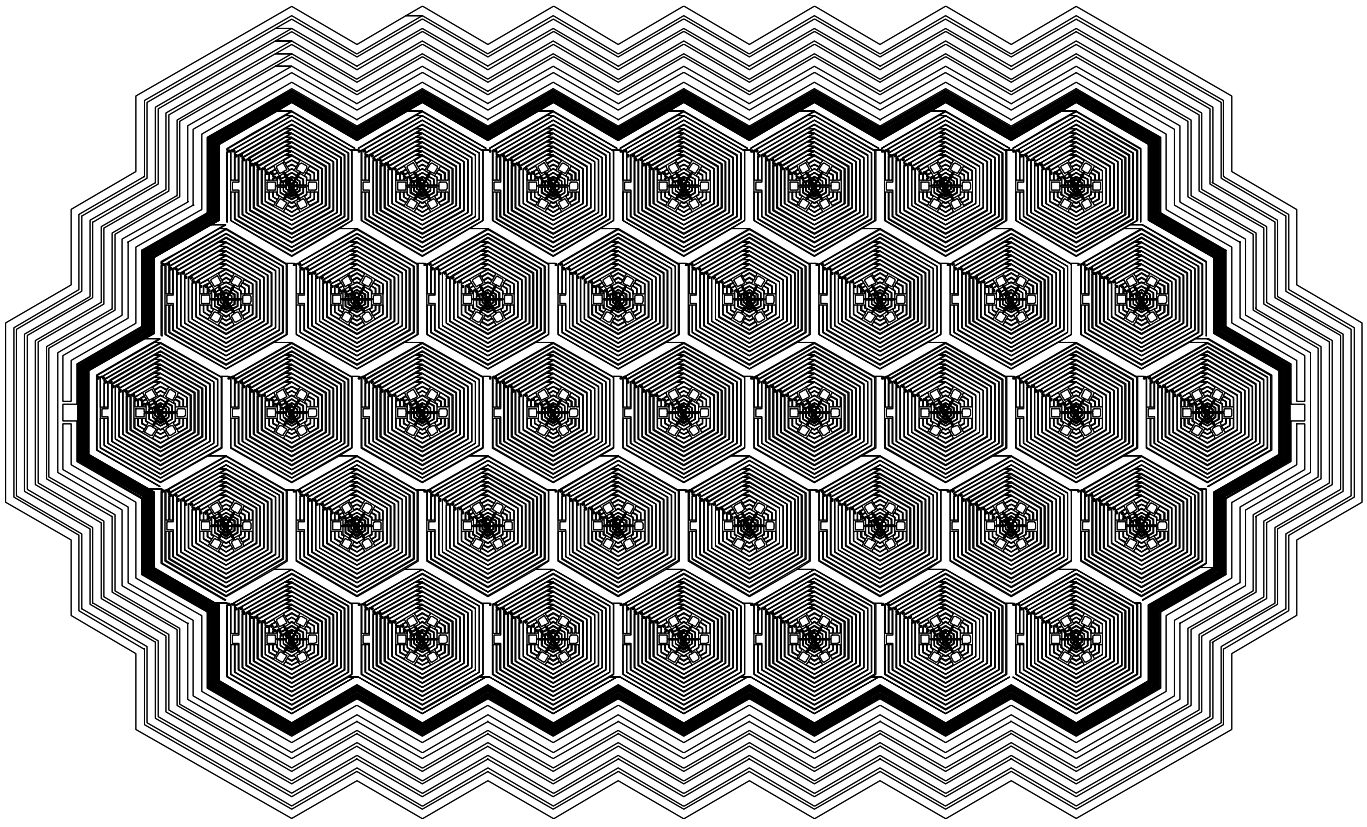

Figure 4: Layout of the 39 cell silicon drift detector array with 39 integrated on-chip amplifiers. The total active size of the system is 195 mm^2.

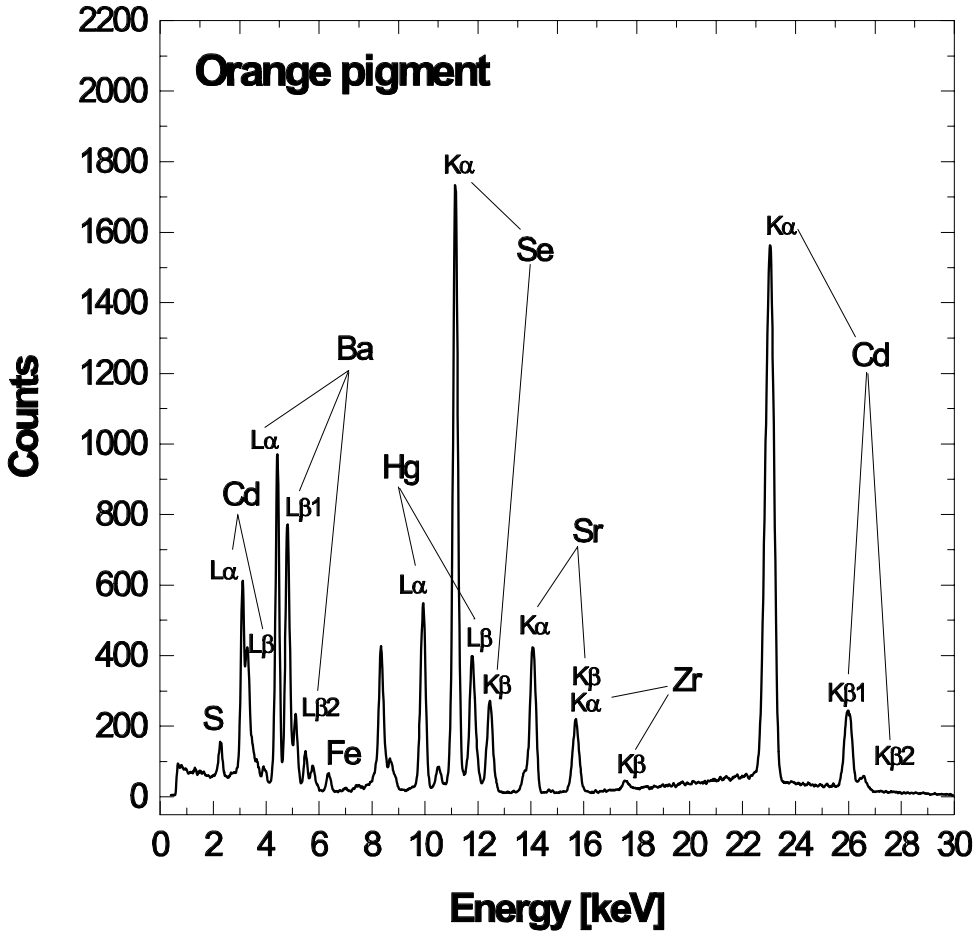

Figure 5: Spectrum of an orange pigment acquired with the XRF-spectrometer based on a Silicon Drift Detector.

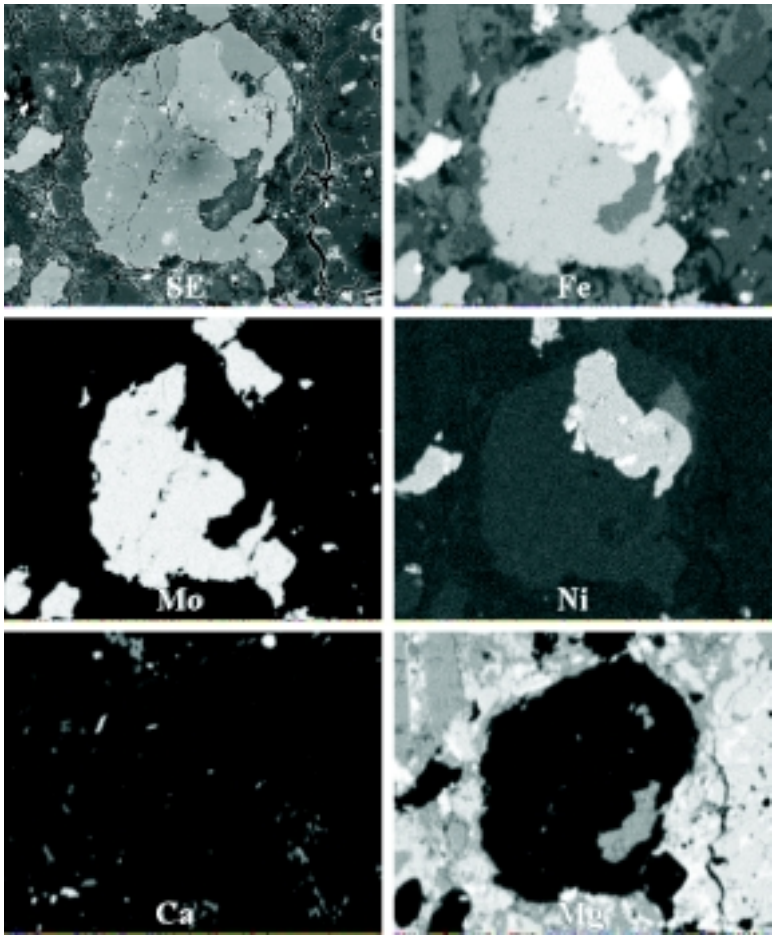

Figure 6: Element imaging with a silicon drift detector. The upper left image shows the topological image with the scanning electron microscope. As inserted in the pictures five element images are shown: Fe, Mo, Ni, Ca and 10 minutes and the average count rate was 250,000 counts per second. The iron image e.g. contains 236 grey steps. The images were processed with a system from Point Electronic^{TM}.

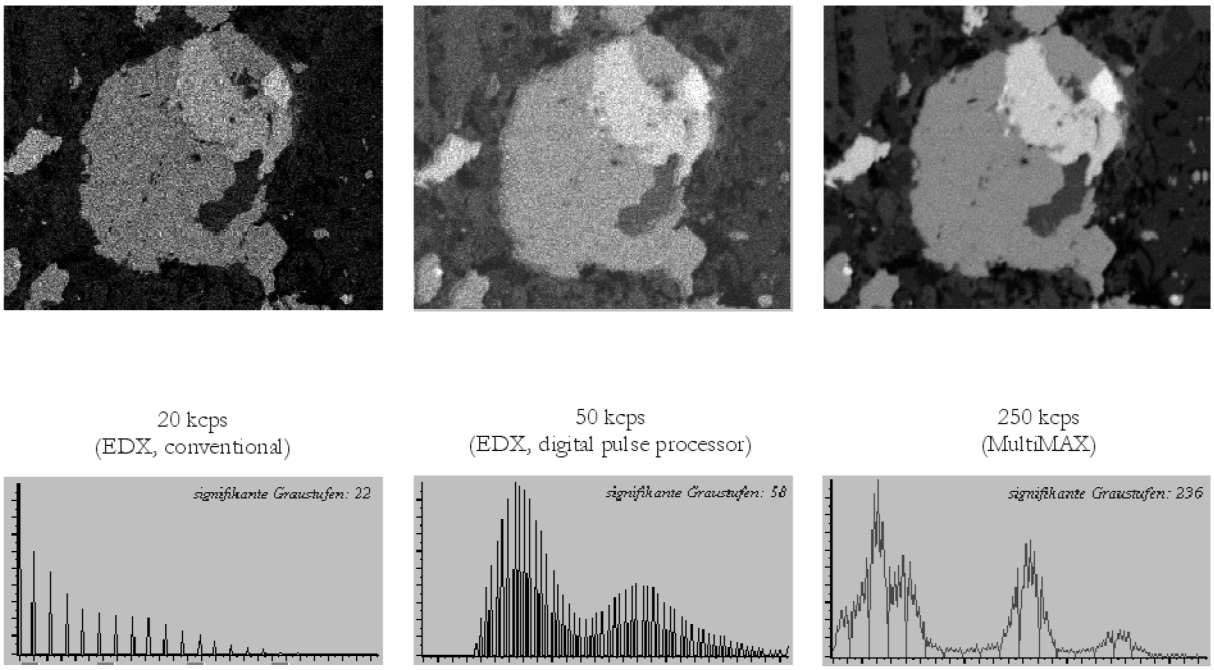

Figure 7: Comparison between a conventional EDX system, a high end digital pulse processor based system and The RÖNTEC-XFlash^{TM} system. The number of grey steps is considerably improved with respect to conventional systems.

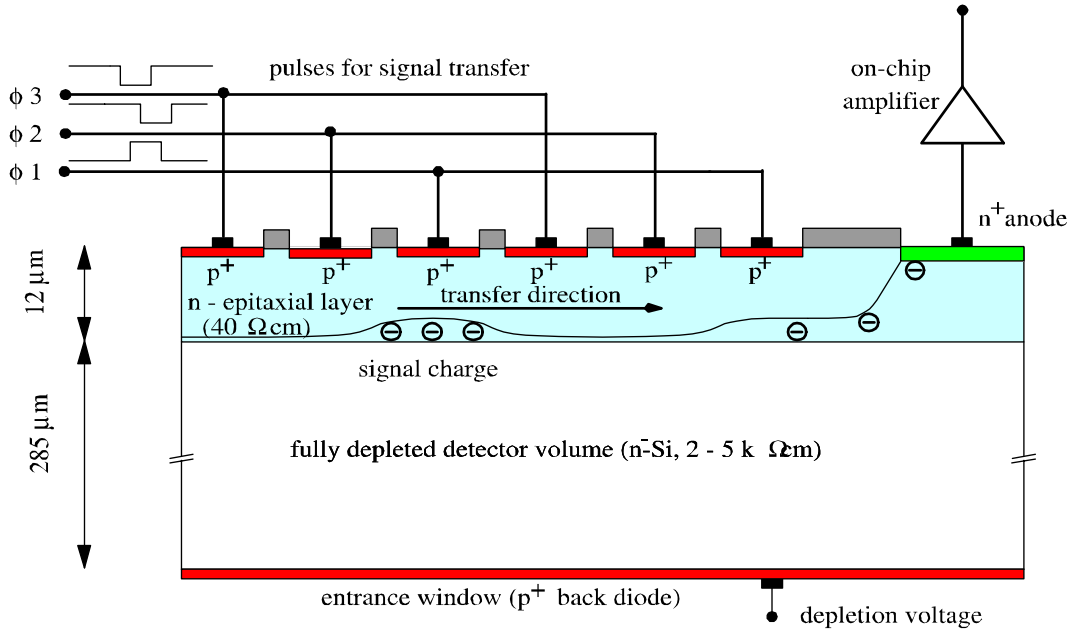

Figure 8: Schematic cross section of a fully sensitive pn-CCD. The radiation enters through the planar thin p^+ back diode. The sensitive thickness is 280μm .

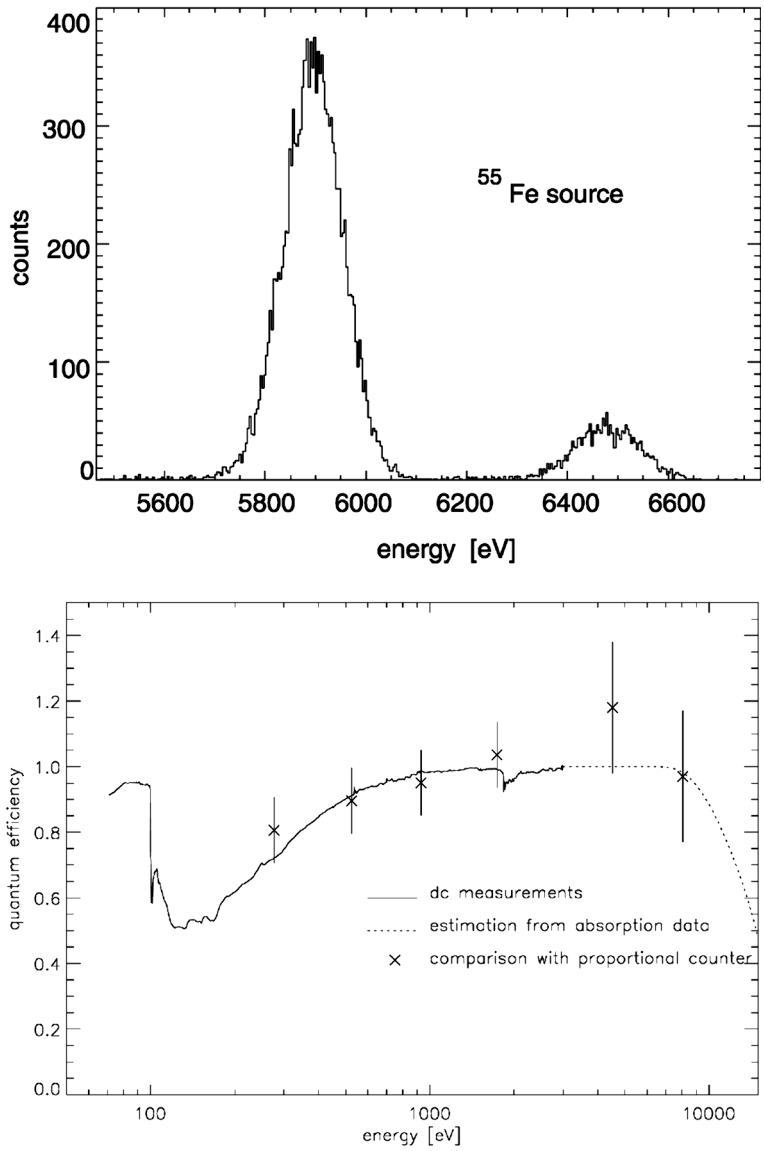

Figure 9: (a) ^{55}Fe spectrum with a pn-CCD in a flat field measurement at a readout speed of 4 ms for a 3× 1 cm^2 large pn-CCD detector. The FWHM of the Mn K_α peak is 130 eV only. (b) shows the measured quantum efficiency in a dc photocurrent measurment (solid line) and in a single photon counting mode (+ signs).

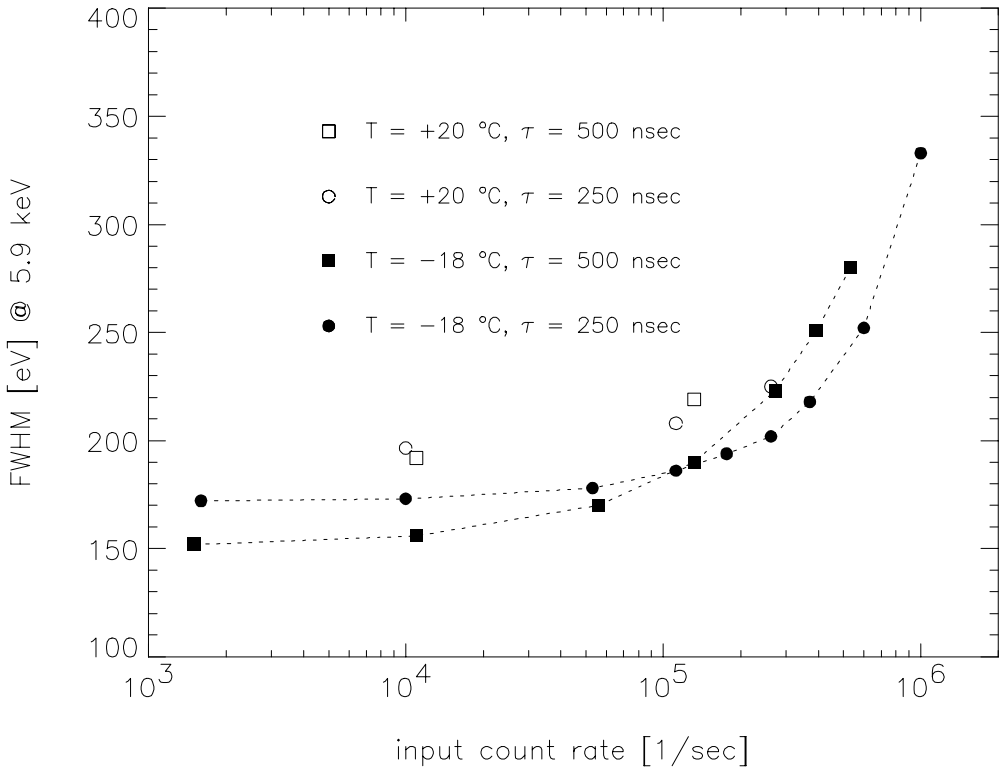

Figure 10: Measurement at room temperature of the count rate dependent energy resolution with an ^{55}Fe source with a silicon drift detector. The measurements were done at shaping times τ = 250ns and τ = 500ns. The operating temperatures were 20 °C (open circles and squares) and -18°C (black circles and squares). At an input count rate of more than 600,000 cps the system 'dead time' was below 30 %. The measured energy resolution with an ^{55}Fe source was 250eV FWHM.